Submitted to Nature Climate Change
A Brief Communication reports a concise study of high quality and broad interest.
(https://www.nature.com/nclimate/content)

Supporting Information to Future Changes in Seasonal Sea-Level Variability Could Reshape Coastal Ecosystems

Tim H. J. Hermans[1], Gregory S. Fivash[2], Jim van Belzen[3,4] *

[1]Institute for Marine and Atmospheric Research Utrecht (IMAU), Utrecht University, Utrecht, The Netherlands
[2]Ecosphere, University of Antwerp, Antwerp, Belgium
[3]Department of Estuarine and Delta Systems, NIOZ – Royal Netherlands Institute for Sea Research, Yerseke, Netherlands
[4]Wageningen Marine Research, Wageningen University and Research, Yerseke, Netherlands

*All authors contributed to the study equally.

ORCIDs:
Tim H. J. Hermans: https://orcid.org/0000-0002-0253-9291
Gregory S. Fivash: https://orcid.org/0000-0002-0767-7036
Jim van Belzen: https://orcid.org/0000-0003-2099-1545

Supplementary note 1 – Sensitivity analysis: Altering the ratio between the amplitudes of the M2 and S2 tidal constituents

The M2 and S2 tidal constituents are characterized by a specific period ($T_{M2} = 12.42\ \mathrm{h}$, $T_{S2} = 12\ \mathrm{h}$). The combination of the two waves produces the 14.76-day spring-neap tide cycle, which causes periodic variance in high and low water levels. The amplitudes of the two tidal constituents vary significantly over the globe, either diminishing or magnifying the amplitude of the spring-neap cycle. Altering the ratio between the amplitudes of the M2 and S2 tidal constituents modifies our predictions of the inundation dynamics experienced under different future scenarios of the annual sea level cycle. Since this effect was ignored in analysis that appears in the main text, we include it here for completeness.

We analyzed the publicly available TICON (*TI*dal *CON*stants) dataset to determine the most globally representative values of $\frac{A_{S2}}{A_{M2}}$. TICON reports the amplitudes of the tidal constituents derived from water level timeseries collected at 1145 tide gauge stations distributed worldwide. The simulations that appear in the main text use the global mean ratio found to be $\frac{A_{S2}}{A_{M2}}$ = 0.4, however this value can vary considerably across the globe: from 0.15 in the 5th-percentile and 0.7 at the 95th-percentile. $\frac{A_{S2}}{A_{M2}}$ has a theoretical range between 0 and 1, where 0 represents a scenario with no spring-neap cycle, and 1 represents the most dominant possible spring-neap cycle where the S2 and M2 tidal constituents are equally prevalent.

We repeated a series of simulations across this range ($0 \leq \frac{A_{S2}}{A_{M2}} \leq 1$), while settling the value of stochastic noise, σ = 0, to separate the independent effect of the $\frac{A_{S2}}{A_{M2}}$ ratio. From these simulations, we find that the amplification of spring-neap tidal cycle (at larger $\frac{A_{S2}}{A_{M2}}$ values) causes an expansion of the spring-neap dominated zone, which correspondingly reduces the width of the twice-daily tidal (intermediate intertidal) zone (Supp. Figure 1).

We used linear regression to estimate the shape of the relationship between a more dominant spring-neap tide, (large $\frac{A_{S2}}{A_{M2}}$), and the position of the zone boundaries (1) where the twice-daily tidal zone transitions to the spring-neap zone $\theta_{S-N}\left(\frac{ASLC_r}{T_r}\right)$, and (2) where the spring-neap zone becomes the annual zone, $\theta_A\left(\frac{ASLC_r}{T_r}\right)$. Here $\theta\left(\frac{ASLC_r}{T_r}\right)$ represents the $\frac{ASLC_r}{T_r}$ required to reach a transition point where two zones meet at mean sea level (see Supp. Figure S1 for visualization).

We found a straightforward, inversely proportional relationship between the value of $\frac{A_{S2}}{A_{M2}}$ and the position of the $\theta_{S-N}\left(\frac{ASLC_r}{T_r}\right)$ transition point, summarized by the following relation:

$$\theta_{S-N}\left(\frac{ASLC_r}{T_r}\right) = 1 - \frac{A_{S2}}{A_{M2}}$$

Meanwhile, the spring-neap/annual transition point has a more complicated asymptotic relationship, described as follows (and see Supp. Figure 2):

$$\theta_A\left(\frac{ASLC_r}{T_r}\right) = 1 + 0.918\,\frac{A_{S2}}{A_{M2}} - 0.519\left(\frac{A_{S2}}{A_{M2}}\right)^2$$

This analysis demonstrates that in systems with a larger spring-neap tidal cycle, the disappearance of the twice-daily intertidal zone will occur with smaller increases in the ASLC. However, the onset of the even more volatile annual cycle-dominated zones that feature months-long inundation/emergence duration events will be delayed. These findings are generally in line with those in our main text, which emphasize how the increase in the amplitude of periodic tidal components creates a more uncertain environment for organisms where disturbances occur more frequently due either to prolonged periods of submergence or emergence, or unexpected extreme events (emergence of the subtidal or flooding of the supratidal).

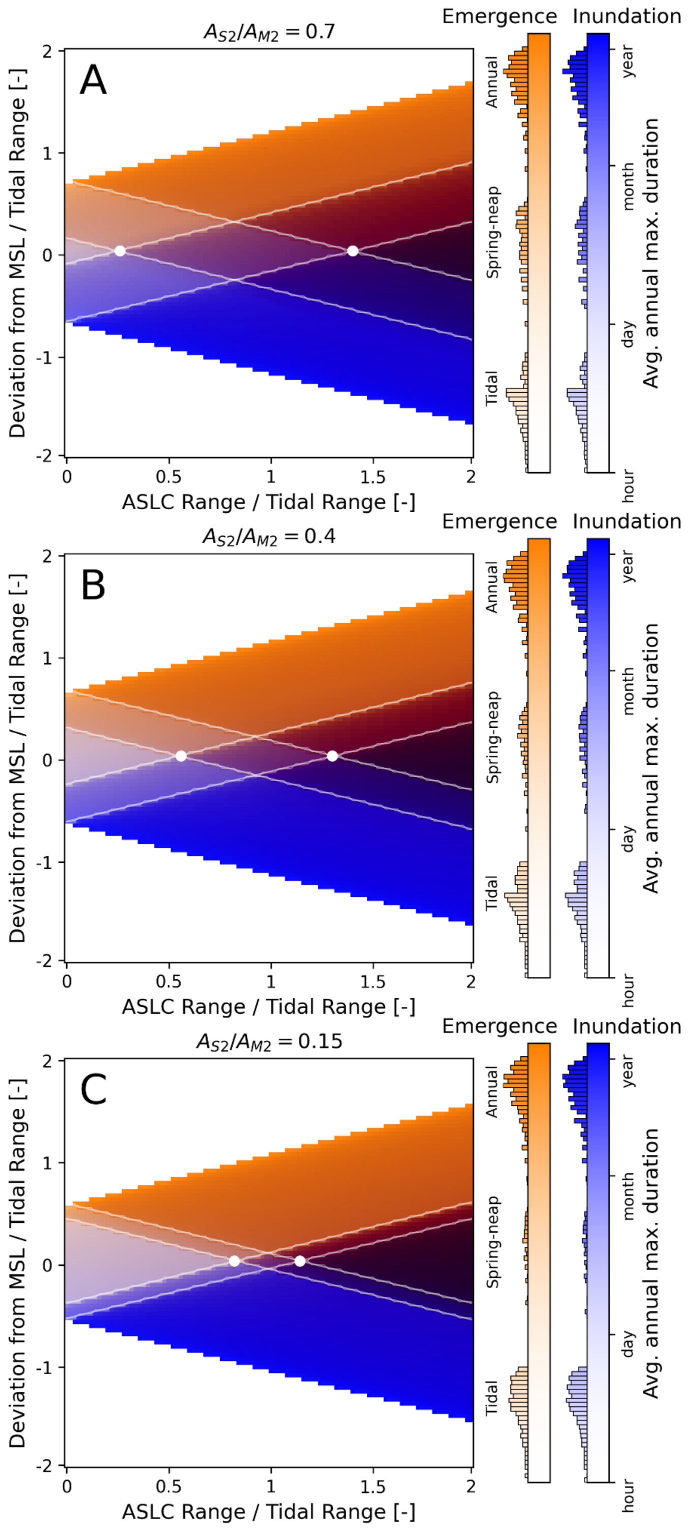

Supplementary Figure 1. These panels show the relative width of the intertidal zone, and the composition of the intertidal zones in three simulated scenarios with varying $\frac{A_{S2}}{A_{M2}}$ ratios: **(a)** 0.15, **(b)** 0.4, and **(c)** 0.70. A larger $\frac{A_{S2}}{A_{M2}}$ ratio leads to a wider variation water levels over the spring neap tide cycle, which leads to (1) a narrower stable intermediate intertidal zone, and (2) an earlier onset of the transition in the intermediate zone from a stable state to a seasonally-transitioning state, under a smaller annual sea-level cycle. The histograms on the colorbars summarize the durations across all elevations and range ratios.

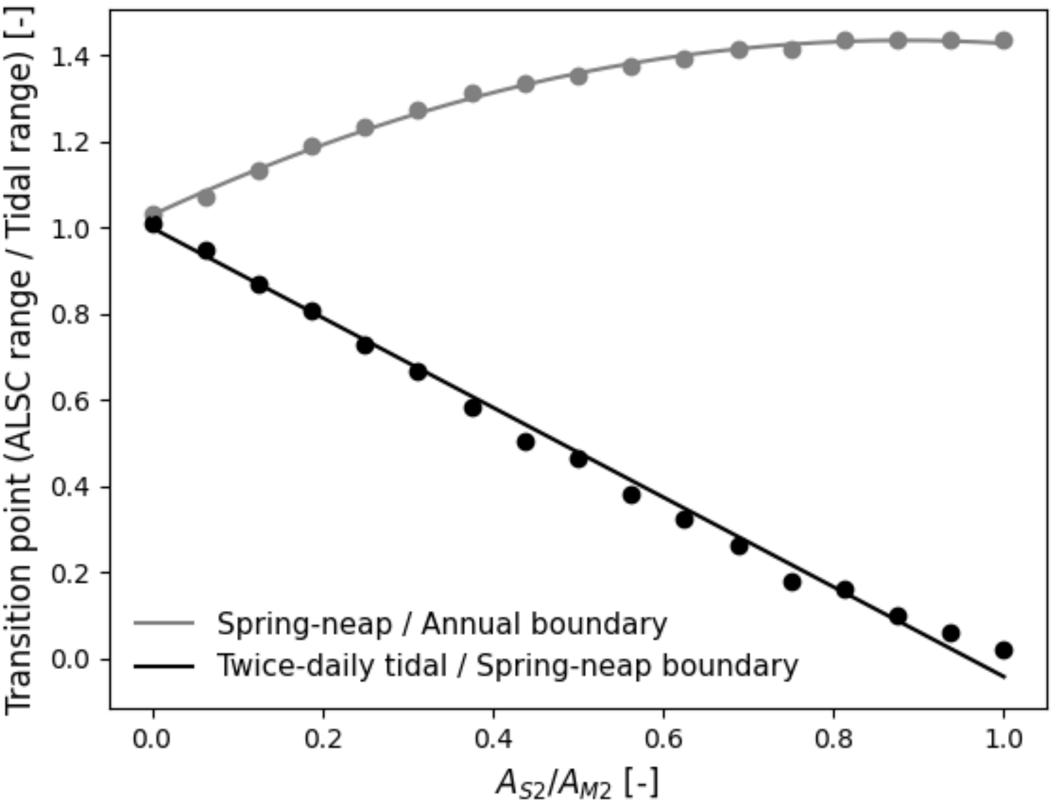

Supplementary Figure 2. Linear regressions showing the relationships between the $\frac{A_{S2}}{A_{M2}}$ ratio and the amplitude of the annual sea-level cycle required for (black) the twice-daily tidal zone to transition to a spring-neap dominated zone, and (grey) the spring-neap zone to transition to an annual cycle-dominated zone at mean sea level.

Supplementary note 2 – Sensitivity analysis: Varying the magnitude of the stochastic tidal constituent

Changes in the stochastic constituent of the tidal water level also affect the width and composition of the intertidal zone. To estimate the effect of the stochastic noise parameters, we varied the standard deviation of the stochastic noise, σ_w, which can be calculated by combining both stochastic parameters, σ and ρ, using the following empirically derived equation:

$$\sigma_w = \frac{\sigma}{\sqrt{2\rho}}$$

In a sequence of simulations, we tested the effect of varying σ_w (between 0 and 0.3) on the position of the transition point where the twice-daily (intermediate intertidal) zone is replaced by the more volatile annual cycle dominated zone, $\theta_A\left(\frac{ASLC_r}{T_r}\right)$. For clarity, we set $\frac{A_{S2}}{A_{M2}}$ = 0, so that the spring-neap tide cycle would not interfere with interpretation of the effect of the stochastic components. We found that much like an amplification of the spring-neap cycle, amplified stochastic variance (predictably) increases the variability of the high and low water levels. Correspondingly, regions where stochastic variability is large will require a smaller amplification of the annual sea level cycle before the twice-daily (intermediate intertidal) zone disappears (Supp. Figure S3). Using linear regression, we determined that the effect of σ_w on the transition point can be quantified by the following formula (Supp. Figure S4):

$$\theta_A\left(\frac{ASLC_r}{T_r}\right) = 1 - 3.2\,\sigma_w$$

Considering the analyses above, we can conclude that the overall volatility of tidal environment can be estimated by considering the additive contributions of stochastic, spring-neap, and annual variations.

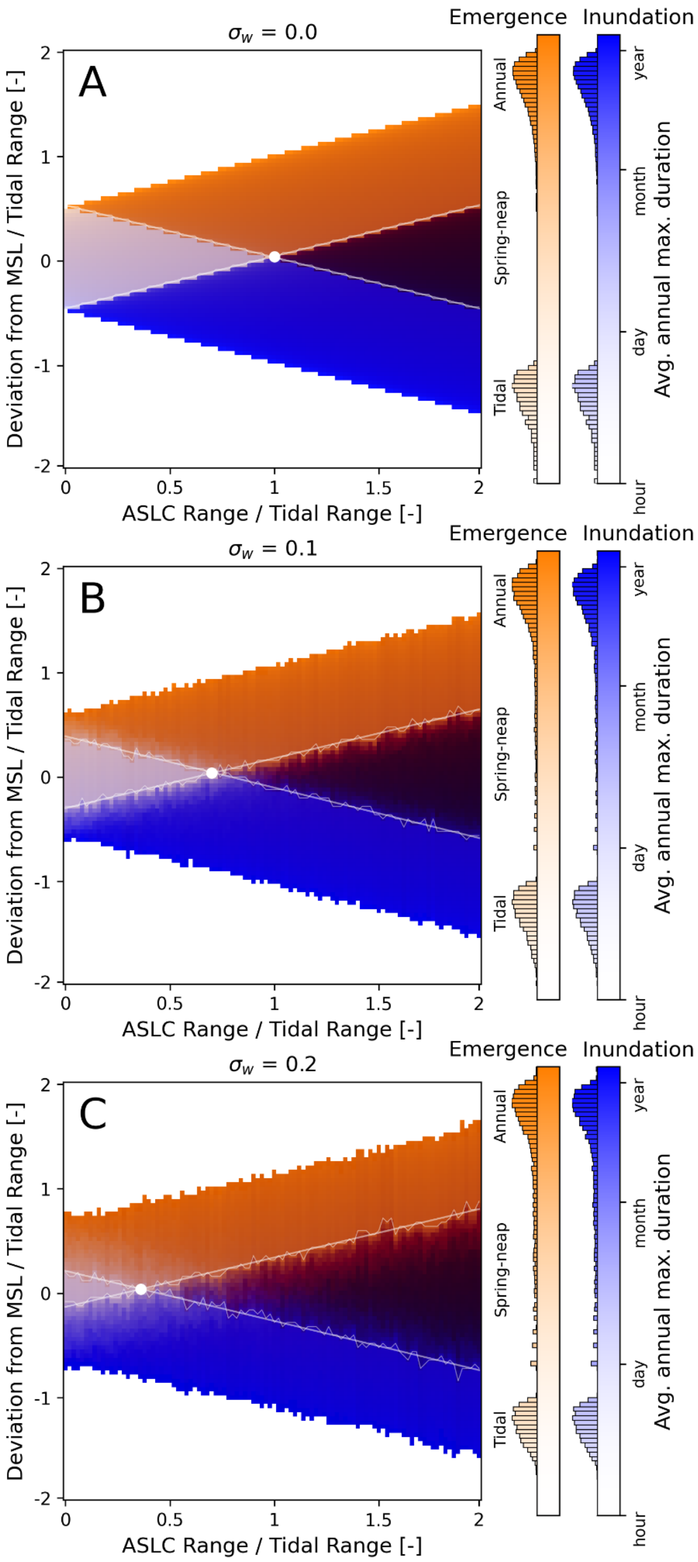

Supplementary Figure 3. These panels show the relative width of the intertidal zone, and the composition of the intertidal zones in three simulated scenarios with varying magnitudes of stochastic noise σ_w: **(a)** 0.00, **(b)** 0.105, and **(c)** 0.211. Larger σ_w values lead to a wider variation in high and low water levels, which leads to (1) a narrower stable intermediate intertidal zone, and (2) an earlier onset of the transition in the intermediate zone from a stable state to a seasonally-transitioning state, under a smaller annual sea-level cycle. The histograms on the colorbars summarize the durations across all elevations and range ratios.

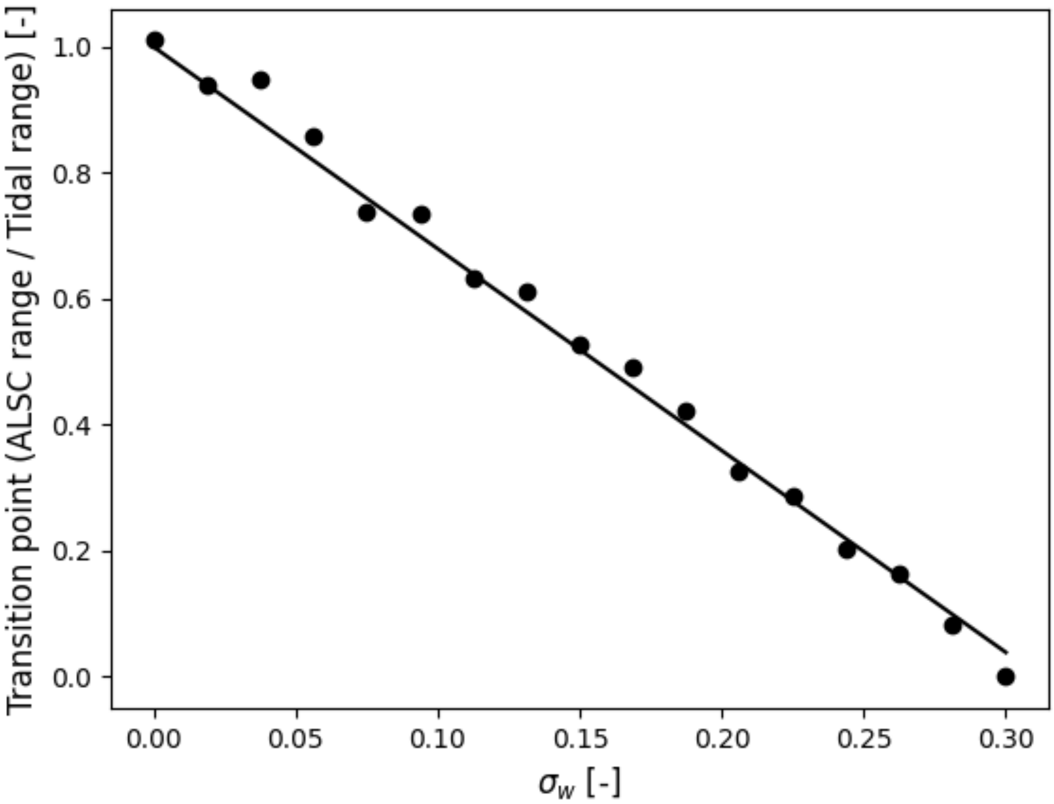

Supplementary Figure 4. Regression showing the relationship between σ_w and the amplitude of the annual sea-level cycle required for the intermediate intertidal zone to transition from a stable state to a seasonally-transitioning state.

Supplementary note 3 – Simulated and Observed Ratios Between the Historical ASLC and Tidal Ranges

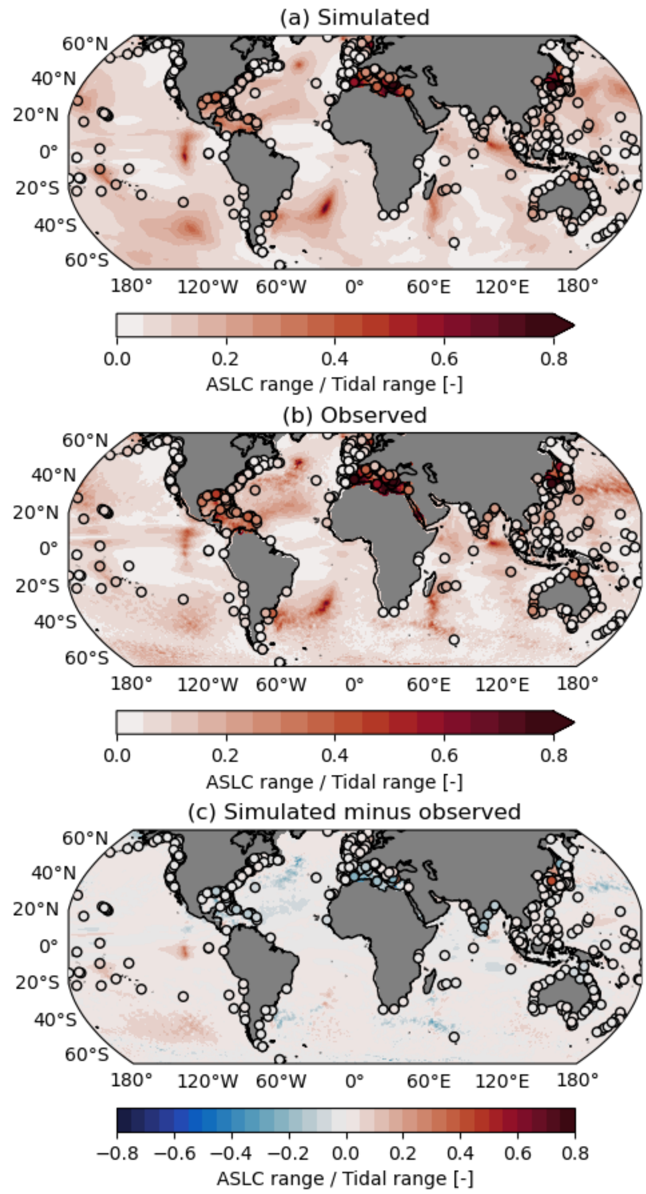

Supplementary Figure 5. (a) the ratio of the range of the historical mean ASLC during 1993-2022 based on CMIP6 simulations (Hermans et al., 2025b) to the historical mean tidal range based on EOT20 (Hart-Davis et al., 2021), as in Fig. 2c, **(b)** the ratio of the range of the historical mean ASLC during 1993-2022 based on satellite and tide-gauge observations (circles) to the historical mean tidal range, **(c)** the CMIP6-based minus the observational ratios.